

**Full title: A Distributed Heat Pulse Sensor Network for Thermo-Hydraulic Monitoring of the Soil Subsurface**

**Abbreviated Title: Distributed Heat Pulse Sensor Network**

Corinna Abesser<sup>1\*</sup>, Francesco Ciocca<sup>2</sup>, John Findlay<sup>3</sup>, David Hannah<sup>4</sup>, Philipp Blaen<sup>4</sup>, Athena Chalari<sup>2</sup>, Michael Mondanos<sup>2</sup> & Stefan Krause<sup>4</sup>

<sup>1</sup> *British Geological Survey, Maclean Building, Crowmarsh Gifford, OX10 8BB, UK*

<sup>2</sup> *Silixa Ltd, Silixa House, 230 Centennial Park, Centennial Avenue, Elstree, WD6 3SN, UK*

<sup>3</sup> *Carbon Zero Consulting, 1C Uppingham Gate, Ayston Road, Uppingham, Rutland, LE15 9NY, UK*

<sup>4</sup> *School of Geography, Earth and Environmental Sciences, University of Birmingham, Edgbaston, Birmingham, B15 2TT, UK*

*\*Correspondence (cabe@bgs.ac.uk)*

**Abstract:**

Fibre optic distributed temperature sensing (DTS) is used increasingly for environmental monitoring and subsurface characterisation. Combined with heating of metal elements embedded within the fibre optic cable, the temperature response of the soil provides valuable information from which soil parameters such as thermal conductivity and soil moisture can be derived at high spatial and temporal resolution, and over long distances.

In this manuscript, we present a novel Active Distributed Temperature Sensing (A-DTS) system and its application to characterise spatial and temporal dynamics in soil thermal conductivity along a recently forested hillslope in Central England, UK. Compared to conventional techniques (needles prob surveys), A-DTS provided values with similar spread though lower on average. The larger number of measurement points that A-DTS provides at higher spatial and temporal resolutions, the ability to repeat surveys under different meteorological/hydrological conditions allows for a more

24 detailed examination of the spatial and temporal variability of thermal conductivities at the study  
25 site. Although system deployment time and costs are higher than with needle probes, A-DTS can be  
26 extremely appealing to applications requiring (1) long term monitoring, (2) at high temporal  
27 repeatability, (3) over long (km) distances and with (4) minimum soil disturbance, rather than one-  
28 off spatial surveys.

29

30 **Keywords:** Distributed temperature sensing, DTS, fibre optic cable, soil thermal conductivity, needle  
31 probe survey, A-DTS, heat pulse, probe method

## 32 Background

33 Detailed knowledge of the ground's thermal properties is essential for process understanding in  
34 many areas in engineering, agronomy, and environmental and soil sciences. In recent years,  
35 considerable efforts have been made to develop methodologies for determining thermal properties  
36 of soils and rocks. One key parameter is thermal conductivity, which is the capacity of a material to  
37 conduct heat. Good knowledge of the thermal conductivity term is required in a variety of  
38 applications, e.g. to design ground source heating/ cooling systems, solar thermal storage, or  
39 underground cable installations.

40 Thermal conductivity is controlled by inherent properties of the geological substrate (texture,  
41 mineral composition) and its transient properties (moisture content, compaction, bulk density and  
42 porosity). Values of thermal conductivity can be calculated from the soil composition using soil  
43 physical models (Côté and Konrad, 2005; Lu et al., 2007) and can also be obtained using laboratory  
44 sample measurements (e.g. Clarke et al. 2008). These methods either require high-resolution soil  
45 data sets (currently not available for the UK) or they alter important soil parameters, such as the in-  
46 situ compaction and bulk density, and hence change the soil thermal properties (e.g. Kersten, 1949).

47 In-situ measurements of thermal conductivity are thus preferable. These can be made by observing  
48 changes in soil temperature in response to natural (i.e. diurnal / seasonal) temperature signal (e.g.,  
49 Busby 2015) or to actively-induced heat flows. This principle is used in classic single-needle heat  
50 pulse probes (Bristow et al. 1994; Campbell et al. 1991) , which use small-diameter thermal needles  
51 with a typical needle length of 0.03–0.10 m (e.g. Decagon Devices 2016; Hukseflux 2017) to  
52 determine soil thermal properties. These measurements are usually only representative of a  
53 relatively small cylinder (0.1 – 0.3 m diameter) of soil around the probe (Decagon Devices 2016;  
54 Hukseflux 2017). A representative assessment of a site's 'bulk' soil conductivity thus requires a  
55 significant number of measurements across a site. King et al. (2012), for example, suggest 12–16  
56 determinations for sites of up to 100 m × 40 m in dimension. However, the measured thermal

conductivities are still only valid at a particular time as these near surface thermal properties are strongly affected by the seasonal variation in soil moisture regime.

Thermal response tests (TRT) are an active, borehole-based method that is widely used in the design of vertical borehole heat exchanger (BHE) systems (e.g. Banks et al., 2013). The tests provides a value of ground bulk thermal conductivity and are considered to be accurate to within 10% (Signorelli et al., 2007). Fibre-optic distributed temperature sensing (DTS) has been used to characterize the vertical distribution of thermal properties within the vertical borehole during a TRT (e.g., Fujii et al. 2009; McDaniel et al. 2018). However, there is at present no equivalent to the vertical borehole TRT for horizontal systems.

Active Distributed Temperature Sensing (A-DTS) employs a similar principle to needle probes, i.e. electrical heating of a fibre-optic (FO) cable while measuring the temperature response along the cable to determine the thermal properties of the surrounding soil. The advantage of this method over the needle heat pulse probe is that it enables the estimation of thermal property distributions along long profiles (e.g. in the order of several kilometres) at spatial resolutions of up to 0.25m. Measurements are easily repeatable; hence the method can also be used to monitor temporal changes in transient soil properties. The concept underlying this A-DTS method is well-established and was successfully proven in controlled laboratory condition, i.e. for artificial systems consisting of homogeneous, bare soils of known mineralogy and soil moisture content (Cao et al. 2015; Ciocca et al. 2012). However, applicability of the method has yet to be demonstrated for actual field –based conditions, which usually are far more complex than those set up in laboratories, with soils consisting of a heterogeneous mix of particle sizes and textures, containing different mineral components, organic matter and water contents, and being covered by different types of vegetation.

In this study, horizontal fibre optic cable loops are deployed at a recently-forested hillslope to test the ability of A-DTS to estimate soil thermal conductivities in natural, heterogeneous field settings where distributions of soil properties, including moisture content, organic matter content and

mineralogical composition are largely variable and unknown. As calibration of the method in a medium of known conductivity is difficult within such complex field settings, we perform a comparison with point measurements made with calibrated thermal needle probes as a way of assessing the validity of our results. This manuscript presents first results from this field application of A-DTS, evaluates results against established needle probe techniques and identifies areas where further study is needed to better understand and improve the performance of the proposed method.

## Study Site

The study site is located in Staffordshire, United Kingdom (Figure 1a), adjacent to the Birmingham Institute of Forest Research (BIFOR) experimental site at Mill Haft (52°47'59"N, 2°18'17"W). The local geology is dominated by the Permo-Triassic Sherwood Sandstone formation, which at the study site, is covered by 10-15 m of superficial deposits, consisting of diamicton / boulder clay (glacial till) and glaciofluvial sand and gravels (Figure 1b). Diamicton is an unsorted, unstratified deposit consisting mostly of a clay and silty clay-dominated matrix with embedded particles that range in size from clay to boulders. It is variable in colour and generally reflects the nature of the source rock material (British Geological Survey, 2018). Grain size variability at the study slope is illustrated in Figure 2, picturing sandy clay (Figure 2b) and boulders (Figure 2c) that were observed in dug pitches at the instrumented slope. Particle size analysis conducted in January 2015 on soil cores that were extracted from up to 1m depth at different locations across the study site confirmed a high clay content (~30% particles <0.063mm) and the presence of small quantities (<10%) of coarser material >2mm (Ciocca et al., 2015).

Current land use at the site consists of a forested plantation along the hillslope, which has been planted in spring 2014 with rows of deciduous saplings (primarily English oak, *Quercus robur*, and sycamore, *Acer pseudoplatanus*), at distances of approximately 1 m between saplings and 1.5 m

between rows. Prior to that, the site was used for arable farming. The mean annual air temperature at the study site is 9°C and mean annual precipitation is 690 mm (Norby et al., 2016).

## Theoretical background

### Measurement principle and key equations

Various methods exist for inferring thermal properties of soils from the temperature response to heating. These are generally based on the solution of the heat conduction equation for a line heat source (or cylindrical heat source) buried in a homogeneous medium – which is the basis for the widely used ‘probe method’ (e.g. Farouki, 1981; Carslaw and Jaeger, 1959). The simplest approximation is to consider the probe as an infinitely long line source of infinitesimal radius, which is uniformly heated and transfers heat energy into a homogeneous and isotropic volume of soil. Such approximation is also valid (within a certain time range) for probes that represent a cylindrical heat source of finite length and finite thickness.

The measurement principle is as follows: (1) An electrical current is applied to the heating elements in the FO cable (or thermal probe) to generate heat (Joule heating) at constant power  $Q$  (W/m) (expressed as power per unit length of heater). (2) The change in temperature  $\Delta T$  (K) is measured as a function of time  $t$  (s) during both the heating phase, that starts when the heater is switched on ( $t=0$ ) and the cooling phase, that starts when the heater is switched off after a time  $t_H$  (s), which is the heat pulse duration. (Note that both, heating and cooling phase can be used independently to estimate the thermal conductivity (e.g. Bristow et al., 1994)). (3) During electrical heating, following a transient period, an asymptotic stage is attained where the measured temperature change  $\Delta T$  (K) approximates a log-linear function, which is directly proportional to the power input  $Q$  (W/m) and inversely related to the soil thermal conductivity  $\lambda$  (W/m K) (Bristow et al., 1994) according to:

$$\Delta T \approx \left( \frac{Q}{4\pi\lambda} \right) (\ln t) + b$$

(Equation 1)

where  $b$  is a constant. (4) Plotting  $\Delta T$  (K) as function of  $\ln(t)$ , the soil thermal conductivity can be calculated from the slope of the straight line, once the log-linearity of  $\Delta T$  (K) (i.e., the asymptotic regime) is attained (Figure 6). The time necessary to reach the asymptotic regime depends on the duration of the transient period, which we refer to in this paper as the *pre-asymptotic stage*.

During the pre-asymptotic stage, the measured temperatures are influenced by the non-ideal thermal characteristics of the probe and the contact resistance between the probe and the soil (Shiozawa and Campbell 1990). This causes temperatures to increase more rapidly than predicted by the log-linear trend in Equation 1 (dotted line in Figure 6). Pre-asymptotic data are generally excluded from the analysis. However, Van der Held and Van Drunen (1949) demonstrated that the introduction of a time correction factor  $t_0$  into Equation 1 can partially compensate for (i) finite thickness of the probe, (ii) thermal contact resistance probe-soil and also (iii) the temporal gap between the beginning of the electrical heating ( $t=0$ ) and the nearest temperature measurement, e.g. in systems where temperature cannot be measured at high sampling rate (e.g. every second or faster). Incorporating  $t_0$  into Equation 1 gives (de Vries, 1952; Shiozawa and Campbell 1990)

$$\Delta T(t) \approx \frac{Q}{4\pi\lambda} \ln(t + t_0)$$

Equation 2

Equation 2 approximates the temperature response to the heating not only during the asymptotic stage (as Equation 1), but already during the pre-asymptotic stage, with a discrepancy from the analytical solution within 5% (Van der Held and Van Drunen, 1949). Typically, the time correction factor  $t_0$  is not known a priori and must therefore be determined from complex laboratory measurements, or estimated from Equation 2 together with the thermal conductivity by means of non-linear regression.

When the pre-asymptotic stage is short, the general approach is to exclude pre-asymptotic data from the analysis and to estimate thermal conductivities by regressing measured temperature

change from the later stages of heating (i.e. the asymptotic stage when data progressively reflect the average characteristics of the surrounding soil (Shiozawa and Campbell 1990)) against  $\ln(t)$  (Bristow et al. 1993), according to Equation 1. For thermal needle probe applications, the duration of this pre-asymptotic period is estimated in good approximation as  $5r^2/\alpha$  (with  $r$  = radius of probe and  $\alpha$  = soil thermal diffusivity) (Hukseflux 2017); typical values are around 70s (King et al. 2012). In A-DTS applications, however, the heated probe (i.e. the FO cable) presents a thicker and more thermally insulated configuration, hence the heating periods required to reach expected asymptotic solution can be much longer. Values of  $> 120$  s (Ciocca et al. 2012) can be expected, especially in dry soils, because of the high thermal contact resistance. Increasing the heat pulse duration to  $> 1000$ s (e.g. as a way of obtaining a long time window of asymptotic data) is not possible because axial heat diffusion within the cable during continuous heating would eventually lead to a noticeable departure from the asymptotic log-linear behaviour as the temperature approaches steady state, instead of following of a monotonic increase with time (Weiss, 2003). Therefore, the possibility to use pre-asymptotic data becomes a critical factor when analysing data from A-DTS applications. From the above discussion, it is obvious that heating strategies, i.e. the applied power and duration of heating periods, are an important aspect of designing measurement programmes for needle probe surveys as well as A-DTS campaigns. A balance must be struck between obtaining meaningful information from both pre-asymptotic and asymptotic stages, avoiding axial heat diffusion and minimising the effects of heating on the soils conditions (i.e. water displacement due to excessive heating (Weiss, 2003) or the development of free convection under conditions of near saturation (Sayde et al. 2014)).

#### Active Distributed Temperature Sensing (A-DTS) method

Distributed Temperature Sensing (DTS) is used by a wide range of applications in environmental monitoring (e.g. Selker et al. 2006) and building observations (e.g. Ferdinand et al. 2014). It utilises the interaction of laser light with the silica core of a fibre-optic cable and applies time-domain reflectometry to determine soil temperature at discrete sections along the cable. During a typical



measurement campaign, the DTS instrument launches short laser pulses at high temporal frequencies along the optical fibre, and measures the backscatter that is generated as the light propagates along the cable. The Raman component of the scattering is temperature-dependent and is used to calculate temperature profiles within the optical fibre (Gratton and Meggitt, 2000; Rose et al., 2013; J. S. Selker et al., 2006). Active Distributed Temperature Sensing (A-DTS), also known as Actively Heated Fibre Optics (AHFO) techniques combine DTS measurements with a heat source, i.e. a metal conductors, embedded within the structure of the cable (Figure 5). Directing an electrical current (e.g. controlled by a variator or a Heat Pulse Control Unit – HPCU) through the metal conductor provides a distributed heat source, which is activated at the same time as temperatures are measured along the FO cable. These temperature data, measured during heating and/or cooling of the cable, reflect the combined efficiency of heat dissipation in the cable and the surrounding medium, allowing spatially distributed estimates of the surrounding thermophysical properties or fluid fluxes to be derived (Aufleger et al., 2000; Bense et al., 2016; PerzImaier et al., 2006, 2004)(Striegl and Loheide, 2012; Weiss, 2003), (Gil-Rodríguez et al., 2012).

Similar to thermal needle probes, the heated fibre optic cable can be conceptualized as a single probe and approximated as a cylindrical heat source of finite length (equal to the length of each spatial sample along the FO) and finite radius. The conductive cores represent the heating elements and the optical fibre the distributed thermometer adjacent to the source (Figure 5). Previous studies analyzed each spatial sample using Equation 1 (e.g. Weiss, 2003). Ciocca et al., (2012) showed that the long heating time required by A-DTS systems to attain the asymptotic stage (up to several minutes in dry soils) leaves only a limited time window for obtaining suitable data. To enable use of pre-asymptotic data, they introduced an iterative method for identifying a threshold time  $t > 0$  during the pre-asymptotic stage after which Equation 2 becomes applicable. The theory is detailed in Ciocca et al., (2012) for both the heating and the cooling phase, and it was successfully applied to calculate distributed thermal conductivities from the cooling phase of A-DTS data collected in a bare, loamy

soil after application of a 120s heat pulse interval. This short pulse duration, however, prevented the application of the modified solution to the heating phase.

In this study, heating times of 900s are applied during A-DTS tests (see Methodology section) to enable the application of the method suggested by Ciocca et al. (2012) to the heating phase data.

## Thermal needle probe method

Thermal needle probe systems are sensor –systems for measuring thermal conductivity and thermal resistivity in sediments and soils. They consist of a probe (“needle”) which incorporates a heating wire and a temperature sensor, and a control /read out unit. Underlying measurement principles and assumptions are based on the transient line-source theory (Carslaw and Jaeger 1959).

Measurements are taken by inserting the probe into the soil at the desired location / depth and allowing needle to equilibrate with the surrounding soil temperature. Once equilibrated, a constant heat flux is generated by applying a voltage to the heating wire in the probe, and the change in temperature  $\Delta T$  (K) at the probe is measured as a function of time  $t$  (s) since start of heating and thermal conductivity is then calculated from the gradient of Equation 1. In these systems, early time data are excluded from the calculation, e.g. the KD2Pro only uses the last 2/3 of collected data (Decagon Devices 2016) while the FTN02 sensor uses the last 1/2 of the measurement cycle for its initial calculations (Hukseflux 2017). This means that effects related to thermal properties of the probe and contact resistance, which influence data collected during early time of heating, can be ignored.

## Methodology

### Active DTS survey

#### Site installation and set up:

Active fibre optic cable loops were installed at the hill slope (Figure 1), centrally between two adjacent rows of trees (slope 1 and slope 2 in Figure 1) and at three different depths (0.40 m, 0.25 m and 0.10 m) below the surface. An armoured, multi-component cable (manufactured by Berk-Tek Inc., US) was used in this study, containing two 18 AWG (America Wire Gauges) insulated copper conductors (electrical resistance = 21  $\Omega$ /km per conductor) (for heating) and two Multi Mode 50/125 $\mu$ m optical fibres (MMF) (for measuring temperature) (Figure 4). The cable was selected for its stability and safety of deployment in field environments. It has an outer diameter (OD) of 0.0077 m and a composite structure (Figure 4). For installation of the FO cables, a soil trench of 500 m [L] x 0.40 m [D] x 0.10 m [W] was excavated in July 2015 (Figure 3a), by means of a hydraulic tracked trencher (Barreto Manufacturing, US). The first cable was laid inside the trench, at 0.40 m depth from the soil surface, and the trench was then carefully backfilled with the previously excavated soils up to a depth of 0.25 m, repeatedly compacting the soil tapping with a flat hammer head and checking for the proper depth before a second fibre optic cable was laid. The operation was repeated at 0.10 m depth for a total of 1,500 m of optical cable buried; the trench was then backfilled with soil (Figure 3b). Conductors for each cable emerging from the trench were wired in parallel and connected to three manual electrical switches in order to lower the total electrical resistance of each cable to 10.5  $\Omega$ /km, and to permit the heating of the cable at a selected depth.

In addition, 15 soil moisture capacitance-based point probes (5-TM, Decagon devices, US) were installed at depths of 0.10 m, 0.25 m and 0.40 m below the soil surface at five different locations along the cable (Figure 1), three at slope 1 (R1, R2, R3 in Figure 1b) and two at slope 2 (L1, L2 in Figure 1b). The probes were connected to battery-powered data loggers (Em50, Decagon Devices, US) for continuous acquisition of soil moisture data at 10 minutes' intervals. The point-capacitance-probe at location R1 and 0.10 m depth developed technical problems during the monitoring period and was therefore not included in the analysis. For the period 01- Jul-2015 – 31-Dec-2015, daily precipitation data were collected from a Met Office tipping bucket (resolution of 0.2 mm) rain gauge (ID 55915, Met-Office, 2017) in approximately 2.12 km distance south-east of the field site. From

January 2016, precipitation was measured at the Mill Haft site, using a tipping bucket (resolution of 0.2 mm). Soil moisture measurements and rainfall data for the study period are shown in Figure 4.

Power supply and instrumentation: The power source was a 7kW, 230V, 32Amps petrol generator (Briggs and Stratton, US). The MMF from all the cable ends were spliced together in three consecutive duplex configurations (e.g. (Hausner et al., 2011; Krause and Blume, 2013)), to form a unique optical path integrating signals sensed in both forward and reverse direction within one single DTS measurement. The A-DTS tests were performed using three DTS instruments (Silixa Ltd, Elstree, UK: (a) a XT-DTS™, 5 km range, 0.25 m sampling resolution; (b) an Ultima-S™, 5 km range and 0.25 m sampling resolution and (c) an Ultima-M™, 10 km range and 0.25 m sampling resolution. The different DTS were set to measure in double-ended configuration (i.e. measurements are performed in sequence half of the time in one direction and half in the opposite, and the temperature is obtained by combining raw data from the two directions) (e.g. Van de Giesen et al., 2012). Double-ended configuration have proved particularly effective to compensate for installation-related drifts in the DTS readings, as for instance introduced by the presence of multiple fusion splices (e.g. van de Giesen et al., 2012). Double-ended measurements also provide the advantage of a temperature resolution that follows a parabolic profile (e.g. van de Giesen et al., 2012), i.e. the resolution is poorer at the near and far ends (i.e. where cable ends are connected to the DTS interrogator ) and is highest towards the mid-range ( i.e. the slope sections).

DTS Measurement campaigns: A total of four A-DTS tests (23 October 2015, 08 June 2016, 09 June 2016 and 25 October 2016) were performed as part of this study. Heating was applied to the cable sections buried in the ground with each individual depth being tested consecutively. The desired electrical current was conveyed to the cables via a Heat Pulse Control Unit (HPCU) (Silixa Ltd, Elstree, UK), which has an embedded high precision power controller (MicroFusion, Control Concepts, US).

The cables were heated sequentially for 900 s, starting with the deepest cable at 0.40 m. Power densities between  $3.3\text{ W m}^{-1}$  and  $5.0\text{ W m}^{-1}$  (in agreement with Striegl and Loheide, 2012) were applied (Table 1) with negligible fluctuations allowed by the HPCU ( $<1\%$ ). Despite the higher rating, the generator could only provide a continuous supply of up to  $2.5\text{ kW}$ , preventing the application of higher pulse intensities (e.g.,  $> 20\text{ W m}^{-1}$ ) as done in previous studies (Ciocca et al., 2012; Sayde et al., 2010). The short heating time (compared for instance to TRT tests lasting days), low power densities applied, and the thermal insulation of the cable, limited the radial thermal footprint to about 0.03 metres (Weiss, 2003) around each cable. This allowed to safely apply a short spacing between the three cable layers to allow investigating thermal conductivity variations at the very top-soil, where many thermal and hydrological processes take place.

Data processing and thermal conductivity calculations: Spatial and temporal interpolation using a piecewise cubic polynomial interpolant (function 'spline', Matlab®) was applied to standardize all data to 0.25 m spatial and 10 s temporal sampling resolution, respectively. The mirrored measurements at each depth were averaged to increase the temperature resolution along the cable. DTS temperature data for the three heated sections were isolated and analysed. The temperature resolution for the XT-DTS at the temporal (10 s) and spatial (0.25 m) sampling applied in this study, over 5km range, is estimated by the manufacturer to vary with a parabolic profile between  $0.35\text{ }^{\circ}\text{C}$  (at 0m and 5,000m) and  $0.20\text{ }^{\circ}\text{C}$  (at 2,500m). In the buried sections analysed, the estimated temperature resolution was  $\leq 0.25\text{ }^{\circ}\text{C}$ . Averaging the mirrored measurements at each depth allowed for a further  $1/\sqrt{2}$  improvement, leading to a temperature resolution of  $\leq 0.18\text{ }^{\circ}\text{C}$  in the buried sections. As the three DTS instrument offer similar performance, this value is also representative for the Ultima-M DTS and Ultima-S DTS.

Distributed thermal conductivity profiles were calculated for the four A-DTS tests by applying the pre-asymptotic approximation method (Ciocca et al., 2012) to the heating phase of each heated DTS

spatial sample according to Equation 2, and performing a robust non-linear fit in Matlab to estimate  $\lambda$  and  $t_0$  simultaneously. The temperatures at  $t=0$  to calculate the  $\Delta T$  (K) during the heating were taken as the average of 120 s of measurements prior to the heating, to reduce any noise in the individual temperature measurement. The threshold time found varied between 60s (wetter soil conditions) and 100s (drier soil conditions) after the beginning of the heating. At such short times, the asymptotic stage was still not reached, and Equation 1 was not yet applicable, hence time corrections were applied (as detailed in the methodology section). All time corrections  $t_0$  were negative and ranged between -55s and -100s, with threshold times longer than those found by Ciocca et al., 2012 for the cooling phase. This is attributed to the longer times required during the heating to approach the asymptotic regime.

#### Needle probe survey

A needle probe survey was conducted on 8th December 2016 to derive thermal conductivities for the site as a means of validating the A-DTS-based method. It had been planned to supplement the needle probe survey with an A-DTS campaign on the following day. However, this was not possible due to problems with the power supply. Therefore, data from a previous A-DTS monitoring campaign (completed on 25 October 2016) had to be used for the comparison, although it is recognised that differing meteorological conditions and soil moistures may mean that the results are not perfectly comparable.

Instruments: The survey was conducted using FTN01 and FTN02 Hukseflux Thermal Sensor systems with single heated needles TP01 (length: 170mm, outer diameter: 6.35 mm) and TP04 (length: 150 mm, outer diameter: 3mm). The needles have a thermal conductivity measurement range of 0.1 to 6 W m<sup>-1</sup> K<sup>-1</sup> and radial footprint of ~100-300 mm (Hukseflux 2017). A KD2Pro Thermal Properties Analyzer system (Decagon Devices 2016) was employed for obtaining more detailed measurements at the depths of FO cable installation at a few sites. The KD2Pro system comes with two sensors, a

single-needle (TR-1) and a dual-needle (SH-1) sensor, and both were employed during the survey. Since TR-1 is optimised for measuring thermal conductivity (while SH-1 is optimised for measuring thermal dispersivity), only data from the single needle sensor TR-1 measurements are considered in this paper. The TR-1 sensor has a length of 100 mm and a diameter of 2.4 mm. It measures thermal conductivity in the range of 0.1 to 4.0 W m<sup>-1</sup> K<sup>-1</sup> with an accuracy of  $\pm 10$ -20% and within a radius of ~30 mm around the probe (Decagon Devices 2016).

Measurement campaign set up: Measurements of thermal conductivity were conducted at 19 locations shown in Figure 1a along the instrumented slope and the surrounding area using the Hukseflux probes. This involved coring a small (~5cm diameter) auger hole into the soil (using a handheld auger) to a depth of 20cm/ 100cm into which the field needle probe was inserted vertically (Figure 5a). Measurement interval of ~20-30cm and ~100-110cm were selected to (1) coincide with the depth of the FO cable installation (at the instrumented slope) (green crosses, Figure 1a) and (2) to be comparable to standardised measurement depths (the base of 100cm auger holes) for BGS thermal conductivity assessments (unpublished data set) for a wider comparison. Measurements were taken at the lower rate of power input (2.34 W m<sup>-1</sup>), applying an equilibration period of 5 min in all cases followed by a heating phase of 5 min (300 s).

A more detailed set of thermal conductivity measurements was taken at four, adjacent sites along the instrumented slope (red triangles, Figure 1a) to test for variations in thermal conductivity between the depths of fibre optic cable installation. Using the KD2Pro Thermal Properties Analyzer system (Decagon Devices 2016), measurements were taken in dug holes at 10cm, 25cm and 40cm depth (matching the depths of cable installation) by inserting the TR-1 Single Needle Sensor horizontally into each measurement horizon (Figure 8b). A monitoring time of 300 seconds was applied for the TR-1, during half of which the sensor was heated while the instrument collected temperature measurements (over full length of read time). A 30-second equilibration period preceded all measurements.

353

## 354 Results

### 355 Thermal conductivity measurements by A-DTS

356 The A-DTS thermal conductivity observations are shown in Figure 7 and summarised in Table 2 for  
357 the different measurement campaigns and cable depths. The plots show that thermal conductivities  
358 vary spatially, with depth as well as with distance along the cable. Localised sharp variations are  
359 evident at a few meters spatial scale, demonstrating the high spatial resolution achievable by the A-  
360 DTS method. Highest thermal conductivities were measured at 10cm depth, ranging between 1.01-  
361 2.20  $\text{W m}^{-1} \text{K}^{-1}$  with geometric means between 1.23 – 1.57  $\text{W m}^{-1} \text{K}^{-1}$  for the different measurement  
362 campaigns. Thermal conductivity ranges were similar at 25cm (0.70-1.88  $\text{W m}^{-1} \text{K}^{-1}$ ) and 40 cm depth  
363 (0.78-2.01  $\text{W m}^{-1} \text{K}^{-1}$ ), but geometric means were somewhat higher at 40cm (1.08-1.36  $\text{W m}^{-1} \text{K}^{-1}$ )  
364 compared to 25cm depth (1.01 – 1.27  $\text{W m}^{-1} \text{K}^{-1}$ ). This is mainly due to a drop in thermal  
365 conductivity around 280-300 m along the cable, i.e. along the middle to upper reaches of slope 2.

366 The data show clear temporal variations in thermal conductivities related to seasonal precipitation  
367 and associated soils moisture changes, with changes in geometric means between different  
368 campaigns of up to 0.34  $\text{W m}^{-1} \text{K}^{-1}$ , 0.26  $\text{W m}^{-1} \text{K}^{-1}$  and 0.28  $\text{W m}^{-1} \text{K}^{-1}$  at 10cm, 25cm and 40cm depth,  
369 respectively. Even the campaigns undertaken on consecutive days (08<sup>th</sup> + 09<sup>th</sup> June 2016) show  
370 considerable variations in thermal conductivity, e.g. changes of up to 0.17 and 0.12  $\text{W m}^{-1} \text{K}^{-1}$  in  
371 maximum and mean (geometric) values are observed at 40cm depth (Figure 7c). Since soil  
372 compaction and mineralogy can be assumed to remain unchanged over the observation period,  
373 these variations are attributed to changes in soil moisture content. However, the exact relationship  
374 between soil moisture and thermal conductivity for soils at the study site is not known. Cosenza et  
375 al. 2003 suggest an increase in thermal conductivity of 0.1  $\text{W m}^{-1} \text{K}^{-1}$  for each 0.1  $\text{m}^3 \text{m}^{-3}$  increase in  
376 soil moisture. Assuming a similar relationship at the soils of the study site, some of the observed  
377 pattern (e.g. thermal conductivities rise of 0.5  $\text{W m}^{-1} \text{K}^{-1}$  between July and October 2016 at 10cm



depth – Figure 7a) cannot be explained by soil moisture changes alone (Figure 4a ), and must be due to some experimental error (as discussed further below).

#### Thermal conductivity measurements by needle probe sensors

Thermal conductivity values measured with the Hukseflux needle probes are shown in Figure 9 and summarized in Table 3 and Figure 10. Values range between 0.83 and 2.63 W m<sup>-1</sup> K<sup>-1</sup> (geometric mean 1.82 W m<sup>-1</sup> K<sup>-1</sup> for n=24). The data show no observable spatial trend. A bulk thermal conductivity for the site of 1.82 W m<sup>-1</sup> K<sup>-1</sup> (geometric mean) is estimated from the (Hukseflux) measurements points (Figure 9). The running arithmetic mean, median and geometric and the 95% confidence interval are plotted (Figure 11) to assess representativeness of the result for the site, as suggested by King et al., (2012). Figure 11 illustrates that 11 and 22 measurements are required to determine bulk thermal conductivity for this site with standard errors of <±15% and <±10%, respectively.

Thermal conductivities measured with the KD2Pro sensor are slightly higher than those obtained using the Hukseflux probes (by approximately 10%), while their standard deviation is smaller. Figure 10a suggests similar median of thermal conductivities at 10cm and 25cm, but a somewhat higher median value at 40cm depth (as measured by the KD2Pro probe). However, observations for the individual horizons are so few (n=4) that it is not possible to draw statistically meaningful conclusions. Thermal conductivities at 25cm and 100cm depths (measured by the Hukseflux probes) also show a small difference in median values, but the overlap in range suggests that the data points belong to the same data population and hence, have the same bulk thermal conductivity.

## Comparison of DTS versus needle probe thermal conductivities

Thermal needle probe data are used in this study as a way of assessing the ability of A-DTS to obtain thermal conductivity in a heterogeneous field setting. Direct comparison of the A-DTS data with data from the needle probe survey are complicated by the fact that the A-DTS campaign and needle probe surveys were not conducted at the same dates, i.e. on 25/10/2016 and 08/12/2016, respectively. Nevertheless, some general observations can be made in comparing the data sets: both data sets, the A-DTS and Hukseflux data show a large degree of variability in thermal conductivities, e.g. due to inhomogeneities in soil composition and porosity, thermal conductivity of the solid fraction and variability of moisture content (Cosenza et al. 2003; King et al. 2012) which can be expected in a heterogeneous deposit such as Boulder clay/ Diamicton (Figure 2). While A-DTS data show a similar degree of dispersion (spread) compared to the needle probe data (Figure 11), the data sets show a statistically significant difference in means ( $p < 0.001$ ), with central values for the A-DTS-derived thermal conductivities being about 25% lower than those obtained by the needle probes. A number of causes may have contributed to the observed differences in measured thermal conductivity ranges between the two methods, as discussed below:

### Soil Conditions

1. Soil moisture changes may have contributed to the discrepancy between the A-DTS measurements, obtained during a period of lower rainfall and soil water contents (Figure 4), and the needle probe measurements, which coincided with a wetter period and higher soil water contents (Figure 4). However, the overall effect of the soil moisture increase ( $0.01 \text{ m}^3 \text{ m}^{-3}$  -  $0.09 \text{ m}^3 \text{ m}^{-3}$ , median  $0.04 \text{ m}^3 \text{ m}^{-3}$ , as measured by the FDR probes) on thermal conductivity is likely to be small, i.e.  $< 0.1 \text{ W m}^{-1} \text{ K}^{-1}$ , assuming an increase in thermal conductivity of  $0.1 \text{ W m}^{-1} \text{ K}^{-1}$  for each  $0.1 \text{ m}^3 \text{ m}^{-3}$  increase in soil moisture (Cosenza et al. 2003).
2. The effect of soil compaction must also be considered as it increases the bulk density and decreases the porosity of a soil, and thus can impact on soil thermal conductivity. For example,

increases in bulk density of  $0.16 \text{ g cm}^{-3}$  (11%) in clay loam and  $0.18 \text{ g cm}^{-3}$  (12%) in sandy loam were found (in a laboratory setting) to result in significant increases in the soil thermal conductivity of up to  $0.27$  (44%) and  $0.83 \text{ W m}^{-1} \text{ K}^{-1}$  (73%), respectively (Abu-Hamdeh 2001). The FO cables were installed in an excavated trench that was backfilled with disturbed soil and then re-compacted (as explained previously). Needle probe measurements were taken adjacent to these refilled trenches and across the wider site. The difference in soil compaction between the refilled and non-disturbed soils may have contributed to the lower thermal conductivity values obtained by the A-DTS during the earlier campaigns (October 2015). However, overall (and specifically during the later campaigns when soils had further compacted) the difference is thought to be relatively minor as, firstly, soil compaction had been applied around and above each cable during installation and, secondly, tree planting activities in 2014, one year prior to the cable installation, are likely to have changed soil bulk density distributions across the site.

#### Fibre optic cable properties and geometry

3. The larger diameter of the fibre optic cable compared to the needle sensor, and the higher thermal resistance due to the presence of an insulation jacket in the cable, instead of bare metal, lead to longer times required for reaching the asymptotic stage (i.e. linearity in temperature increase as a function of natural logarithm of time). According to Ciocca et al., (2012), the heating is slower than the cooling phase to reach the log-linear regime. Witte et al., (2002) gives a heating time of  $t \geq 5r^2/\alpha$ , where  $r$  is the cable radius in meters and  $\alpha$  the thermal diffusivity of the jacket in  $\text{m}^2 \text{ s}^{-1}$ , for log-linear conditions to be reached. Assuming a thermal diffusivity of PVC ( $\alpha=8e^{-8} \text{ m}^2 \text{ s}^{-2}$ ) and a radius  $r=0.0035\text{m}$ , linearity is attained after 750s. Therefore, the solution in Equation 2 may not be sufficient to compensate for the use of data from the pre-asymptotic (transient) stage in the processing, leading to an underestimation of the computed thermal conductivities.

4. Figure 5 shows the arrangements of components within the DTS cable. From that, it is obvious that the assumption of a cylindrical source within the soil is not strictly met when using the DTS cable. Hence, the underlying assumption of the probe method are not fully adhered to, and this may impact on the derived solution. In another study, the influence of the thermal conductivity of the outer sheath material (which was lower than that of the surrounding medium) was suggested to have contributed to the underestimation of thermal conductivities measurements by the DTS (Sakaki et al. 2019).

#### Power supply limitations

5. The petrol generator only allowed for a maximum power rate of 5W/m. Although other A-DTS investigations used similar power inputs for soil moisture measurements (Striegl and Loheide, 2012), it may be too low for the specific cable design adopted in this study. The positive correlation between power input and the accuracy of A-DTS-derived measurements has been demonstrated by Dong et al (2017) for soil moisture measurements. Furthermore, the power output from a petrol generator is unavoidably less constant/ stable compared to a mains power source, and fluctuations in the applied power rate during the heating phase are likely to have added to the experimental uncertainty; e.g. it is believed to be the main reason for the observed variability during consecutive survey as in June 2016 (Figure 7c). The system has since been connected to mains power, and is currently being retested.

#### Instrument characteristics

6. The observed differences in thermal conductivity values produced by the different methods may be attributable to the difference in soil volumes over which measurements are integrated. Assuming a radial footprint of 100-300mm for the Hukseflux, the measured volume for the needle probes is between 4 – 40 L. There are no data yet available on the volume of soil influenced by the heating of the fibre optic cable, but the radial footprint of FO cable is estimated to be < 30 mm around the cable (Weiss, 2003). At distances greater than that the

temperature increase becomes smaller than the instrument temperature resolution. The measured volume of soil per DTS spatial sample (0.25m) is therefore  $\leq 1$  L. The heating time required to expand the footprint to be comparable with the needle probes would introduce axial diffusion effects, making the A-DTS technique not applicable. The limited footprint allows for a fine horizontal characterization of the soil, identifying variability into centimetres-thick layers. Differences in measured soil volume may also be responsible for the variability in measured thermal conductivities between the Hukseflux and the KD2Pro sensors of about  $\pm 10$  %. However, the obtained precision is generally consistent with findings from an inter-laboratory study, which indicated a measurement precision of between  $\pm 10$  and  $\pm 15$  % for different needle probes, and identified a general tendency to a positive bias (higher value) over the known values for the materials studied (ASTM 2000).

#### Uncertainty assessment and calibration:

7. Temperature resolution of the measurements along the installed cable was tested and was found to follow the parabolic curve typical for double ended configuration with lower resolution of  $0.35$  °C at the cable ends (at 0m and 5,000m) and highest resolution of  $0.20$  °C along the mid-section of the cable (at 2,500m). The averaging of the mirrored temperatures per each depth allowed for a further improvement of a  $1/\sqrt{2}$  factor in the buried section, with resolution  $\leq 0.18$  °C. Calibration for thermal conductivity ( $\lambda$ ) was not undertaken for the A-DTS installation presented in this study. However, calibration and detailed error analysis of the method has been carried out in a previous study, and validity of the approach was proven in a setting of known soil properties and thermal conductivity distribution as described in Ciocca et al., (2012). Uncertainties in  $\lambda$  were found to be  $< 6\%$  for their method, as used in this study but applied to the cooling phase. However, cable geometry and heating strategies differ within each field application, and the calibration coefficients vary along the cable depending on surrounding soil properties and moisture conditions. An absolute calibration, as done for needle probes (e.g. by

means of measurements on substance of known thermal conductivity), is not possible for such field application due to the scale and size of the installation and the fact that field settings are largely variable and unknown. In conventional TRT tests, for example, observed water temperature variations are fitted with a mathematical model (often the line-source model) to estimate the thermal properties of the subsurface and the borehole that forms part of the borehole heat exchanger installation. As there is no “reference” ground with known characteristics, on-site calibration of the method and uncertainty assessment are usually not possible. Recently, the concept of an aboveground virtual borehole has been suggested to calibrate TRT units for different ground thermal conditions and conductivities (Corcoran et al. 2019), or factorial analysis has been carried out to assess the uncertainty associated with the measurements (Raymond et al. 2011), but such assessments remain rare in the context of TRTs.

## Discussion

A-DTS permits repeated interrogation of soil properties at the exact same locations using active or passive measuring modes. It, therefore, has utility for detailed monitoring of changes in soil properties, e.g. in response to external stresses, such as plant water uptake, climate change or repeated heating/ cooling associated with ground source heat pump and heat storage operations. For the determination of thermal conductivities for ground source heat pump applications, it is generally recommended that measurements should be taken during dry periods to derive a conservative estimate (King et al, 2012), but little consideration is given to the temporal variability of thermal conductivities. Here we present some preliminary findings from four A-DTS campaigns. The data suggest that thermal conductivities at the study slope vary by up to 30% between the measurement campaigns, with variations of up to 10% occurring between consecutive days. However, these findings are based on 4 measuring campaigns only, subject to the inherent experimental uncertainty discussed above. Some of these uncertainties have now been addressed, e.g. by replacing the generator with a mains power source. Furthermore, longer-term A-DTS

526 monitoring with sequential (mains powered) heating of 900 s per depth has since been undertaken  
527 at 6 hours intervals, to further test repeatability of measurements and assess changes in soil thermal  
528 conductivity and soil moisture with different approaches. These new data sets are currently being  
529 analysed and will provide further insight into the temporal dynamics in thermal conductivity at the  
530 daily and the seasonal scale. Such knowledge could inform operational strategies for ground source  
531 heat application, specifically optimisation of system efficiencies.

532 By providing high spatial and temporal resolution data over long time and large spatial extents, A-  
533 DTS methods have the potential to serve as an “across the scale” tool that can fill the gap between  
534 point sensors (high-frequency measurements at small spatial footprints) and remote techniques  
535 such as COSMOS and satellites observations (low-frequency measurements at large, averaged  
536 footprints and shallow penetration depths). At this intermediate scale, spatial coverage and  
537 resolution provided by the DTS method, i.e. 0.25m-spaced measurements over 1.5km of heated  
538 cable, remains unprecedented.

539 Certainly, the monitoring objective must be such that installation times of several weeks and costs of  
540 several tens of thousands GBP (for instrumentation and installation) can be justified. Measurements  
541 of thermal conductivities, e.g. for the design of routine ground heat application, will not require an  
542 A-DTS installation, except where detailed temperature/ thermal conductivity monitoring of the  
543 installation during operation is of interest. In most of these standard cases, needle probe surveys  
544 offer a much more cost and time-effective method, and it has been confirmed in this study that  
545 representative estimates of bulk thermal conductivity can be obtained with comparatively little  
546 effort, i.e. requiring 22 needle probe measurements to yield an estimate of the bulk thermal  
547 conductivity representative of conditions at the study site (on the day measurements were taken)  
548 and with errors <10%.

549 However, for applications requiring (1) long term monitoring, (2) at high temporal repeatability, (3)  
550 over long distances and (4) with minimum soil disturbance, the A-DTS provides an extremely valuable

tool. Leak detection along pipelines, dams and infrastructures, or in-situ monitoring of soils to optimise irrigation of agricultural crops, are examples where A-DTS may lead to critical benefits that justify cost and installation effort.

Further work is needed to better understand the heat transfer processes within the innovative cable geometries such as the one applied in this study, and to improve data analysis techniques. Modelling of the heat transfer within a complex structure as the heated FO cable by means of advanced software (e.g. Comsol Multiphysics) should be performed in order to provide critical insights on the actual temperature increase of the soil compared to the core of the cable, the radial footprint, the timescales involved and the optimal power rate required, improving the applicability of the A-DTS technique. The high density of measurements may supply local temperature, thermal conductivity and soil moisture data, which can then be converted into information relating to heat and water fluxes in the subsurface. Such data can be used to drive and/or validate eco-hydrological models, contributing to critically-needed improvements in smart-irrigations techniques; ground source heat pump optimisation and heat storage system designs, as well improving leak detection from sensitive infrastructures such as sewers and water pipes, or oil and gas pipelines.

Further testing and validation of the method is required, including simultaneous A-DTS and Needle Probe campaigns as well as an assessment of the impact of different heating strategies on the surrounding soil. This will permit the optimisation of the method, balancing power input against accuracy of thermal conductivity estimations, as well as provide an assessment of the measurement footprint of the method.

## Conclusions

This study has demonstrated that active DTS has the potential to provide a promising alternative for measuring thermal conductivity at the field scale at high spatial and temporal resolutions. Active DTS produced results within the range of thermal needle probe measurements in terms of spread of the



values, although with statistically significant lower central values. Further testing and improvements are required that address the experimental uncertainties inherent in the methodology and set up applied in this study.

While initial installation of the A-DTS system is more time consuming and expensive than a needle probe survey (but similar in cost to a standard TRT), it has some key advantages: (1) the methods can provide distributed measurement for horizontal BHE systems (as opposed to TRTs which are currently only available for vertical BHE systems), (2) it provides spatially-distributed thermal conductivities instead of a single bulk value, and (3) measurements are easily repeatable. The latter can be of particular advantage where the temporal variability in thermal properties due to changing soil moisture conditions or the influence of groundwater flow on heat transport and thermal properties needs to be assessed.

A number of factors have been identified that may have affected the thermal conductivity estimations at the A-DTS. The impact of these factors on the overall measurement precision has not been investigated in detail, and further studies are necessary to better understand these effects and to optimise method operational parameters and analysis.

## Acknowledgement

This research is part of the Distributed Heat Pulse Sensor network for subsurface monitoring of heat and water fluxes project (DiHPS). We acknowledge the support from the project advisory board which includes BIFoR – the Birmingham Institute for Forestry Research, the European Space Agency (ESA), Carbon Zero Consulting, the UK Forestry Commission and the UK Soil Moisture Observation Network (COSMOS-UK). We are grateful to Carbon Zero Consulting, specifically to Laurence Scott, for their support with the needle probe survey. We publish with the permission of the Executive Director of the British Geological Survey (UKRI). The authors declare that they have no conflict of

599 interest. We thank the anonymous reviewers for the many insightful comments and suggestions that  
600 improved the quality of the manuscript.

## 601 Funding information

602 The DiHPS project is funded by the UK Natural Environmental Research Council (NERC). The project  
603 has received further support from the INTERFACES FP7-PEOPLE-2013-ITN and HiFreq HORIZON 2020-  
604 PEOPLE-2016-RISE.

## References

- Abu-Hamdeh, N.H. 2001. SW—Soil and Water: Measurement of the Thermal Conductivity of Sandy Loam and Clay Loam Soils using Single and Dual Probes. *Journal of Agricultural Engineering Research*, 80, 209-216, doi: <https://doi.org/10.1006/jaer.2001.0730>.
- Abu-Hamdeh, N.H. & Reeder, R.C. 2000. Soil Thermal Conductivity Effects of Density, Moisture, Salt Concentration, and Organic Matter. *Soil Science Society of America Journal*, 64, 1285-1290, doi: 10.2136/sssaj2000.6441285x.
- Aufleger, M., Strobl, T., Dornstadter, J., 2000. Fiber optic temperature measurements in dam monitoring – four years of experience, in: *ICOLD Congress Q78*, R.1, Beijing.
- Banks, D., Withers, J.G., Cashmore, G., Dimelow, C., 2013. An overview of the results of 61 in situ thermal response tests in the UK 46, 281–291. doi:10.1144/qjegh2013-017
- Bense, V.F., Read, T., Bour, O., Le Borgne, T., Coleman, T., Krause, S., Chalari, A., Mondanos, M., Ciocca, F., Selker, J.S., 2016. Distributed Temperature Sensing as a downhole tool in hydrogeology. *Water Resour. Res.* 52, 9259–9273. doi:10.1002/2016WR018869
- Bristow, K., White, R. & Kluitenberg, G. 1994. Comparison of single and dual probes for measuring soil thermal properties with transient heating. *Soil Research*, 32, 447-464, doi: <https://doi.org/10.1071/SR9940447.7>
- Bristow, K.L., Campbell, G.S. & Calissendorff, K. 1993. Test of a heat-pulse probe for measuring changes in soil water content. *Soil Science Society of America Journal*, 57.
- British Geological Survey: The BGS Lexicon of Named Rock Units, Result Details: Diamicton, [www.bgs.ac.uk](http://www.bgs.ac.uk), accessed 17 August 2019.
- Busby, J. 2015. Determination of thermal properties for horizontal ground loop collector loops. *Proceedings World Geothermal Congress Melbourne, Australia*, 19-25 April 2015.

628 Campbell, G.S., Calissendorff, C. & Williams, J.H. 1991. Probe for measuring soil specific heat using a  
629 heat-pulse method. *Soil Science Society of America Journal*, 55.

630 Carslaw, H.S., Jaeger, J.C., 1959. *Conduction of Heat in Solids*. Oxford University Press, Oxford, UK.

631 Ciocca, F., Krause, S., Chalari, A., Mondanos, M., 2015. Fibre Optics Distributed Temperature Sensing  
632 for EcoHydrological Characterization of a Complex Terrain, in: *European Geosciences Union*  
633 (EGU) General Assembly 2015.

634 Ciocca, F., Lunati, I., Van de Giesen, N., Parlange, M.B., 2012. Heated Optical Fiber for Distributed  
635 Soil-Moisture Measurements: A Lysimeter Experiment. *Vadose Zo. J.* 11.  
636 doi:10.2136/vzj2011.0199

637 Clarke, B.G., Agab, A. & Nicholson, D. 2008. Model specification to determine thermal conductivity of  
638 soils. *Proceedings of the Institution of Civil Engineers - Geotechnical Engineering*, 161, 161-168,  
639 doi: 10.1680/geng.2008.161.3.161.

640 Cosenza, P., Guérin, R. & Tabbagh, A. 2003. Relationship between thermal conductivity and water  
641 content of soils using numerical modelling. *European Journal of Soil Science*, 54, 581-588, doi:  
642 10.1046/j.1365-2389.2003.00539.x.

643 Côté, J., Konrad, J.-M., 2005. A generalized thermal conductivity model for soils and construction  
644 materials. *Can. Geotech. J.* 42, 443–458. doi:10.1139/t04-106

645 de Vries, D., Peck, A., 1958. On the Cylindrical Probe Method of Measuring Thermal Conductivity  
646 with Special Reference to Soils. I. Extension of Theory and Discussion of Probe Characteristics.  
647 *Aust. J. Phys.* 11, 255. doi:10.1071/PH580255

648 Decagon Devices. 2016. *KD2 Pro Thermal Properties Analyzer*.

649 Dong, J., Agliata, R., Steele-Dunne, S., Hoes, O., Bogaard, T., Greco, R. & van de Giesen, N. 2017. The  
650 Impacts of Heating Strategy on Soil Moisture Estimation Using Actively Heated Fiber Optics.  
651 *Sensors*, 17, 2102.

652 Farouki, O. 1981. Thermal properties of soils. United States Army Corps of Engineers, Cold Regions  
653 Research and Engineering Laboratory.

654 Ferdinand, P., Giuseffi, M., Roussel, N., Rougeault, S., Fléchon, O. & Barentin, V. 2014. Monitoring  
655 the energy efficiency of buildings with Raman DTS and embedded optical fiber cables. SPIE.

656 Fujii, H., Okubo, H., Nishi, K., Itoi, R., Ohyama, K. & Shibata, K. 2009. An improved thermal response  
657 test for U-tube ground heat exchanger based on optical fiber thermometers. *Geothermics*, 38,  
658 399-406, doi: <https://doi.org/10.1016/j.geothermics.2009.06.002>.

659 Gil-Rodríguez, M., Rodríguez-Sinobas, L., Benitez-Buelga, J., Sanchez-Calvo, R., 2012. Application of  
660 active heat pulse method with fiber optic temperature sensing for estimation of wetting bulbs  
661 and water distribution in drip emitters. *Agric. Water Manag.* 120, 72–78.

662 Gratton, K.T.V., Meggitt, B.T., 2000. *Optical Fiber Sensor Technology*. Kluwer Academic Publishers,  
663 Boston, MA.

664 Hausner, M.B., Suárez, F., Glander, K.E., van de Giesen, N., Selker, J.S., Tyler, S.W., 2011. Calibrating  
665 single-ended fiber-optic raman spectra distributed temperature sensing data. *Sensors* 11,  
666 10859–10879. doi:10.3390/s111110859

667 Hukseflux. 2017. User Manual FTN02 Field Thermal Needle System for Thermal Resistivity /  
668 Conductivity Measurement.

669 King, W., Banks, D. & Findlay, J. 2012. Field determination of shallow soil thermal conductivity using  
670 a short-duration needle probe test. *Quarterly Journal of Engineering Geology and*  
671 *Hydrogeology*, 45, 497-504, doi: 10.1144/qjegh2012-002.

672 Krause, S., Blume, T., 2013. Impact of seasonal variability and monitoring mode on the adequacy of  
673 fiber-optic distributed temperature sensing at aquifer-river interfaces. *Water Resour. Res.* 49,  
674 2408–2423. doi:10.1002/wrcr.20232

675 Krause, S., Blume, T., Cassidy, N.J., 2012. Investigating patterns and controls of groundwater up-  
676 welling in a lowland river by combining Fibre-optic Distributed Temperature Sensing with  
677 observations of vertical hydraulic gradients. *Hydrol. Earth Syst. Sci.* 16, 1775–1792.  
678 doi:10.5194/hess-16-1775-2012

679 Krause, S., Tecklenburg, C., Munz, M., Naden, E., 2013. Streambed nitrogen cycling beyond the  
680 hyporheic zone: Flow controls on horizontal patterns and depth distribution of nitrate and  
681 dissolved oxygen in the upwelling groundwater of a lowland river. *J. Geophys. Res.*  
682 *Biogeosciences* 118, 54–67. doi:10.1029/2012JG002122

683 Lu, S., Ren, T., Gong, Y., Horton, R., 2007. An Improved Model for Predicting Soil Thermal  
684 Conductivity from Water Content at Room Temperature. *Soil Sci. Soc. Am. J.*  
685 doi:10.2136/sssaj2006.0041

686 McDaniel, A., Tinjum, J., Hart, D.J., Lin, Y.-F., Stumpf, A. & Thomas, L. 2018. Distributed thermal  
687 response test to analyze thermal properties in heterogeneous lithology. *Geothermics*, 76, 116-  
688 124, doi: <https://doi.org/10.1016/j.geothermics.2018.07.003>.

689 Norby, R.J., De Kauwe, M.G., Domingues, T.F., Duursma, R.A., Ellsworth, D.S., Goll, D.S., Lapola, D.M.,  
690 Luus, K.A., MacKenzie, A.R., Medlyn, B.E., Pavlick, R., Rammig, A., Smith, B., Thomas, R.,  
691 Thonicke, K., Walker, A.P., Yang, X., Zaehle, S., 2016. Model-data synthesis for the next  
692 generation of forest free-air CO<sub>2</sub> enrichment (FACE) experiments. *New Phytol.* 209, 17–28.  
693 doi:10.1111/nph.13593

694 Perzmaier, S., Aufleger, M., Conrad, M., 2004. Distributed fiber optic temperature measurements in  
695 hydraulic engineering - Prospects of the heat-up method, in: *Proceedings of the 72nd ICOLD*  
696 *Annual Meeting Workshop on Dam Safety Problems and Solutions-Sharing Experience*, Korean  
697 *Natl. Comm. on Large Dams*, 16-22 May, Seoul, Korea.

698 Perzmaier, S., Straer, K.H., Strobl, T., Aufleger, M., 2006. Integral seepage monitoring on open

699 channel emabnkment dams by the DFOT heat pulse method, in: Proceedings of the 74th  
700 Annual Meeting, Int. Comm. on Large Dams, Barcelona, Spain.

701 Raymond, J., Therrien, R., Gosselin, L. & Lefebvre, R. 2011. A Review of Thermal Response Test  
702 Analysis Using Pumping Test Concepts. *Groundwater*, 49, 932-945, doi: 10.1111/j.1745-  
703 6584.2010.00791.x.

704 Rose, L., Krause, S., Cassidy, N.J., 2013. Capabilities and limitations of tracing spatial temperature  
705 patterns by fiber-optic distributed temperature sensing. *Water Resour. Res.* 49, 1741–1745.  
706 doi:10.1002/wrcr.20144

707 Sayde, C., Gregory, C., Gil-Rodriguez, M., Tufillaro, N., Tyler, S., van de Giesen, N., English, M.,  
708 Cuenca, R., Selker, J.S., 2010. Feasibility of soil moisture monitoring with heated fiber optics.  
709 *Water Resour. Res.* 46, n/a-n/a. doi:10.1029/2009WR007846

710 Sayde, C., Thomas, C.K., Wagner, J., Selker, J., 2015. High-resolution wind speed measurements using  
711 actively heated fiber optics. *Geophys. Res. Lett.* 42, 10,064-10,073. doi:10.1002/2015GL066729

712 Selker, J., van de Giesen, N., Westhoff, M., Luxemburg, W., Parlange, M.B., 2006. Fiber optics opens  
713 window on stream dynamics. *Geophys. Res. Lett.* 33, L24401. doi:10.1029/2006GL027979

714 Selker, J.S., Thévenaz, L., Huwald, H., Mallet, A., Luxemburg, W., van de Giesen, N., Stejskal, M.,  
715 Zeman, J., Westhoff, M., Parlange, M.B., 2006. Distributed fiber-optic temperature sensing for  
716 hydrologic systems. *Water Resour. Res.* 42, n/a-n/a. doi:10.1029/2006WR005326

717 Shiozawa, S. & Campbell, G.S. 1990. Soil thermal conductivity. *Remote Sensing Reviews*, 5, 301-310,  
718 doi: 10.1080/02757259009532137.

719 Signorelli, S., Bassetti, S., Pahud, D., Kohl, T., 2007. Numerical evaluation of thermal response tests.  
720 *Geothermics* 36, 141–166. doi:https://doi.org/10.1016/j.geothermics.2006.10.006

721 Striegl, A.M., Loheide, S.P., 2012. Heated distributed temperature sensing for field scale soil

722 moisture monitoring. *Ground Water* 50, 340–7. doi:10.1111/j.1745-6584.2012.00928.x

723 Tyler, S.W., Selker, J.S., Hausner, M.B., Hatch, C.E., Torgersen, T., Thodal, C.E., Schladow, S.G., 2009.

724 Environmental temperature sensing using Raman spectra DTS fiber-optic methods. *Water*

725 *Resour. Res.* 45. doi:10.1029/2008WR007052

726 van de Giesen, N., Steele-Dunne, S.C., Jansen, J., Hoes, O., Hausner, M.B., Tyler, S., Selker, J., 2012.

727 Double-ended calibration of fiber-optic raman spectra distributed temperature sensing data.

728 *Sensors (Switzerland)* 12, 5471–5485. doi:10.3390/s120505471

729 Van der Held, E.F.M., Van Drunen, F.G., 1949. A method of measuring the thermal conductivity of

730 liquids. *Physica* 15, 865–881. doi:doi:10.1016/0031- 8914(49)90129-9

731 Weiss, J.D., 2003. Using Fiber Optics to Detect Moisture Intrusion into a Landfill Cap Consisting of a

732 Vegetative Soil Barrier. *J. Air Waste Manage. Assoc.* 53, 1130–1148.

733 doi:10.1080/10473289.2003.10466268

734 Westhoff, M.C., Savenije, H.H.G., Stelling, G.S., Selker, J.S., Pfister, L., Uhlenbrook, S., 2007. A

735 distributed stream temperature model using high resolution temperature observations. *Hydrol.*

736 *Earth Syst. Sci.* 125–149.

737 Witte, H.J.L., van Gelder, G.J. & Spitler, J.D. 2002. In Situ Measurement of Ground Thermal

738 Conductivity: A Dutch Perspective. *ASHRAE Transactions*, **108**, 263-273.

739

740



## Tables

Table 1: Details of the A-DTS tests performed between October 2015 and October 2016

Survey date	Power Density	DTS sampling	DTS time	DTS model
	$Q$		interval	
[dd/mm/yy]	[W m <sup>-1</sup> ]	[m]	[s]	
23/10/15	3.3±1%	0.25	20	XT-DTS
08/06/16	3.7±1%	0.25	10	Ultima-M
09/06/16	4.8±1%	0.25	10	Ultima-M
25/10/16	5.0±1%	0.125*	10	Ultima-S

Table 2: Statistical analysis of thermal conductivities  $\lambda$  (W m<sup>-1</sup> K<sup>-1</sup>) from A-DTS at the different cable depths. \*Data were spatially interpolated for the analysis to get the same spatial sampling of 0.25m

	23/10/2015	08/06/2016	09/06/2016	25/10/2016	Maximum difference in $\lambda$ between campaigns
10cm depth					
n	1928	1928	1928	1928	
Minimum	1.02	1.01	1.02	1.29	0.28
<b>Median</b>	<b>1.29</b>	<b>1.21</b>	<b>1.25</b>	<b>1.56</b>	<b>0.35</b>
Maximum	1.66	1.70	1.80	2.20	0.50
Arithmetic mean	1.30	1.23	1.27	1.58	0.35
Standard deviation	0.11	0.11	0.12	0.14	0.03
<b>Geometric mean</b>	<b>1.29</b>	<b>1.23</b>	<b>1.26</b>	<b>1.57</b>	<b>0.34</b>
25cm depth					
n	1928	1928	1928	1928	
Minimum	0.70	0.70	0.70	0.78	0.08
<b>Median</b>	<b>1.13</b>	<b>1.01</b>	<b>1.02</b>	<b>1.29</b>	<b>0.28</b>
Maximum	1.62	1.53	1.56	1.88	0.35
Arithmetic mean	1.11	1.02	1.03	1.28	0.26

Standard deviation	0.15	0.16	0.16	0.17	0.02
<b>Geometric mean</b>	<b>1.10</b>	<b>1.01</b>	<b>1.02</b>	<b>1.27</b>	<b>0.26</b>
40cm depth					
n	1928	1928	1928	1928	
Minimum	0.93	0.78	0.85	1.00	0.21
<b>Median</b>	<b>1.25</b>	<b>1.09</b>	<b>1.20</b>	<b>1.35</b>	<b>0.26</b>
Maximum	1.83	1.64	1.81	2.01	0.37
Arithmetic mean	1.26	1.09	1.21	1.37	0.28
Standard deviation	0.14	0.13	0.16	0.14	0.03
<b>Geometric mean</b>	<b>1.25</b>	<b>1.08</b>	<b>1.20</b>	<b>1.36</b>	<b>0.28</b>

Table 3: Summary of thermal conductivities  $\lambda$  (W m<sup>-1</sup> K<sup>-1</sup>) from (a) Hukseflux and (b) KD2Pro needle probes and (c) A-DTS campaign on 25/10/2016

	(a) Hukseflux (all data)	(b) KD2Pro (all data)	(c) A-DTS 25/10/2016 (all data)
n	24	12	5784
Minimum	0.83	1.76	0.78
<b>Median</b>	<b>1.88</b>	<b>2.02</b>	<b>1.39</b>
Maximum	2.63	2.82	2.02
Arithmetic mean	1.87	2.09	1.41
Standard deviation	0.45	0.27	0.20
<b>Geometric mean</b>	<b>1.82</b>	<b>2.07</b>	<b>NA</b>

## **List of Figures**

Figure 1: (a) Location (inset), land use and set up of the study site, (b) Geology of superficial deposits at the study site (Contains Digital geological data, British Geological Survey ©NERC. Contains Ordnance Data © Crown Copyright and database rights [2017]. Ordnance Survey Licence no. 100021290)

Figure 2: Photos of (a) the instrumented slope 2 years after cable installation, and (b) sandy clays and (c) boulder in clay matrix encountered along the slope in dug pits during the needle probe survey

Figure 3: (a) Trenched slope during installation of fibre optic cable (inset) and (b) instrumented slope and A-DTS instrument enclosure (inset) immediately after completion of cable installation

Figure 4: Rainfall and soil moisture data for the study period. Dotted lines mark dates of A-DTS campaigns (blue) and needle probe survey (green).

Figure 5: Cross section of the heated fibre optic cable

Figure 6: Example of Ciocca et al (2012) iterative approach to determine the applicability of Equation 2 for the calculation of thermal conductivity. Temperature evolution (blue line) during heating of sample number 175 (44m) at 0.40cm depth during the A-DTS test of October 23, 2015 is shown, together with the thermal conductivities calculated using different measurements at  $t > 0$  (the arrows indicate the first point of each fit). After a threshold time of  $\sim 50$ s, the consecutive values do not show significant variations, Equation 2 is considered applicable.

Figure 7: Thermal conductivities from the different A-DTS tests at 10cm (a), 25cm (b), and 40cm (c) depth

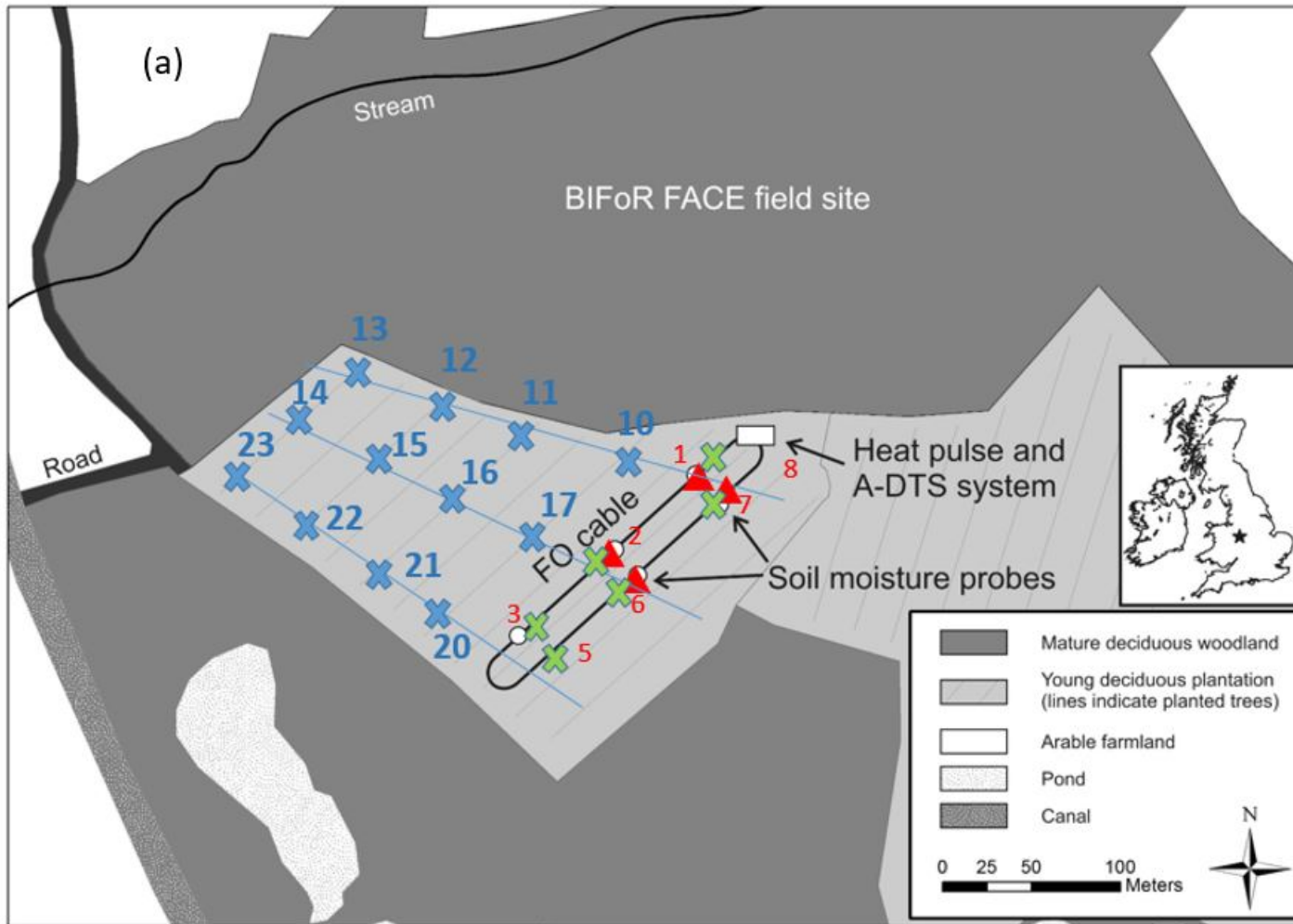
Figure 8: Deployment of thermal needle probes during survey on 08 December 2016: (a) Hukseflux FTN01/02 field thermal needle system (Needle vertically inserted for bulk measurements at 25cm

774 and 100cm depth.) and (b) KD2Pro Thermal Properties Analyzer with TR-1 Single Needle Sensor  
775 (inset) (Needle horizontally inserted for measurements of 10cm, 25cm and 40cm soil horizon). The  
776 dual-needle probe of the KD2 was not used for this study.

777 Figure 9: Distribution of thermal conductivities measured by Hukseflux FTN01/02 thermal needle  
778 system at depths of cm.

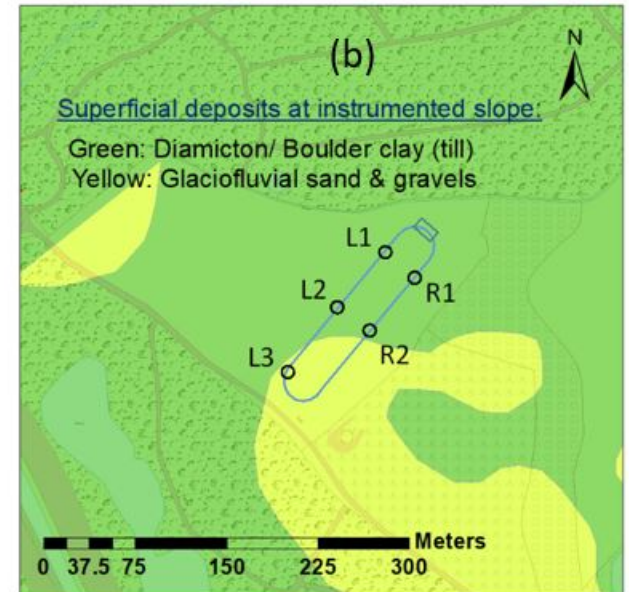
779 Figure 10: Whisker plot of thermal conductivities measured by (a) needles probes and (b) A-DTS on  
780 25/10/2016 at different depth horizons

781 Figure 11: Plot of arithmetic mean, median, geometric mean and 95% limits of confidence against  
782 number of measurements for successive needle probe (Hukseflux) determinations.



✕ ✕ **Auger hole measurements**  
(Hukseflux) & soil sampling  
Depths: 100cm , (30cm)

▲ **Measurements on dug profile**  
(KD2Pro probes) & soil sampling  
Depths: 10cm, 25cm, 40cm

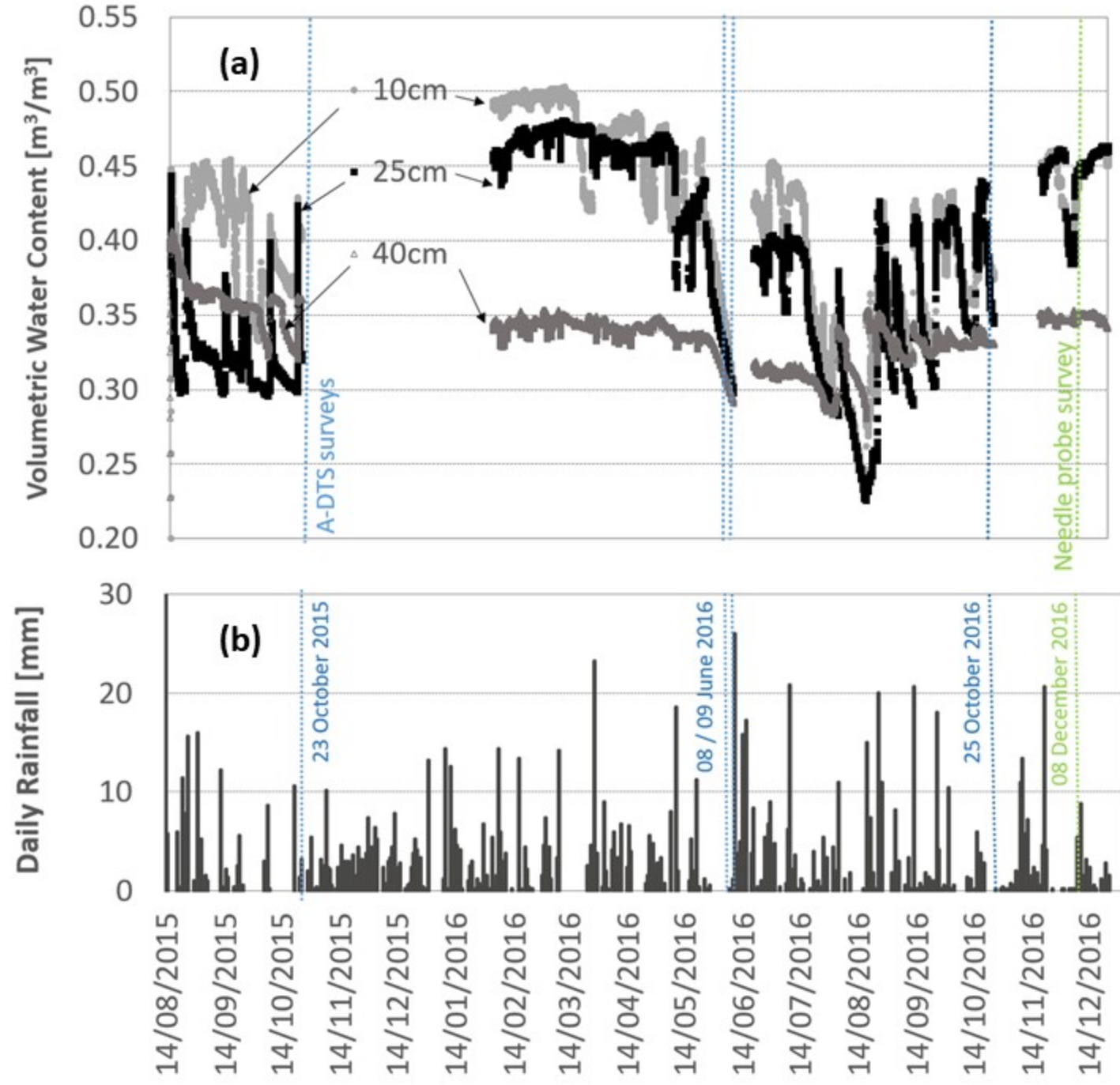






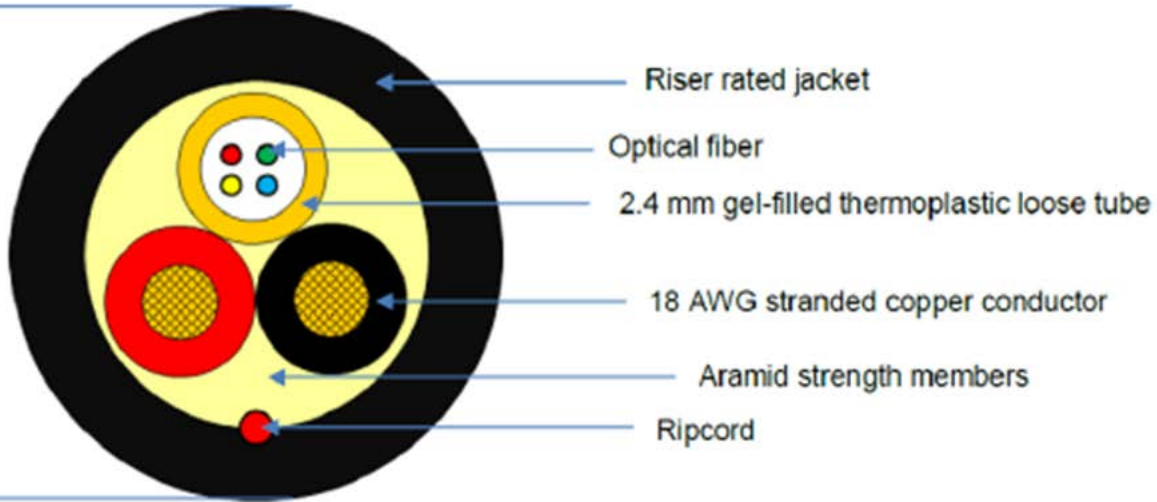


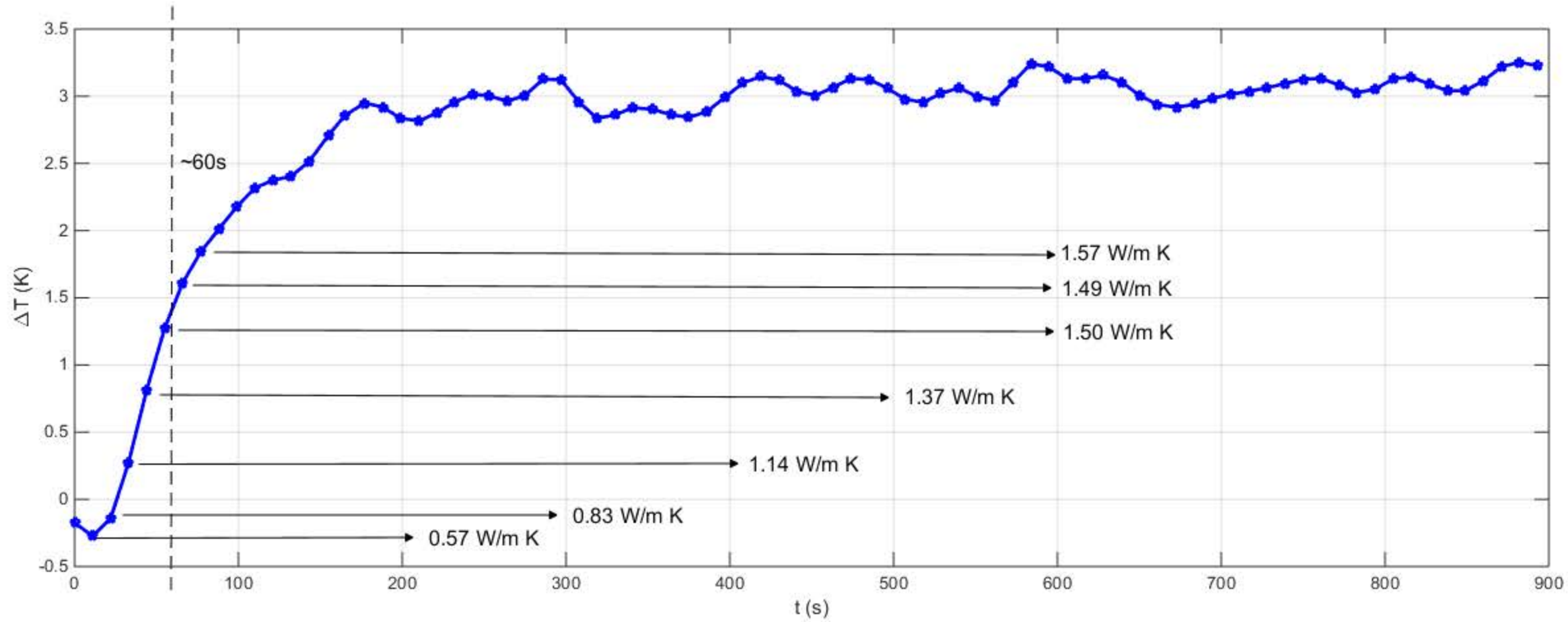




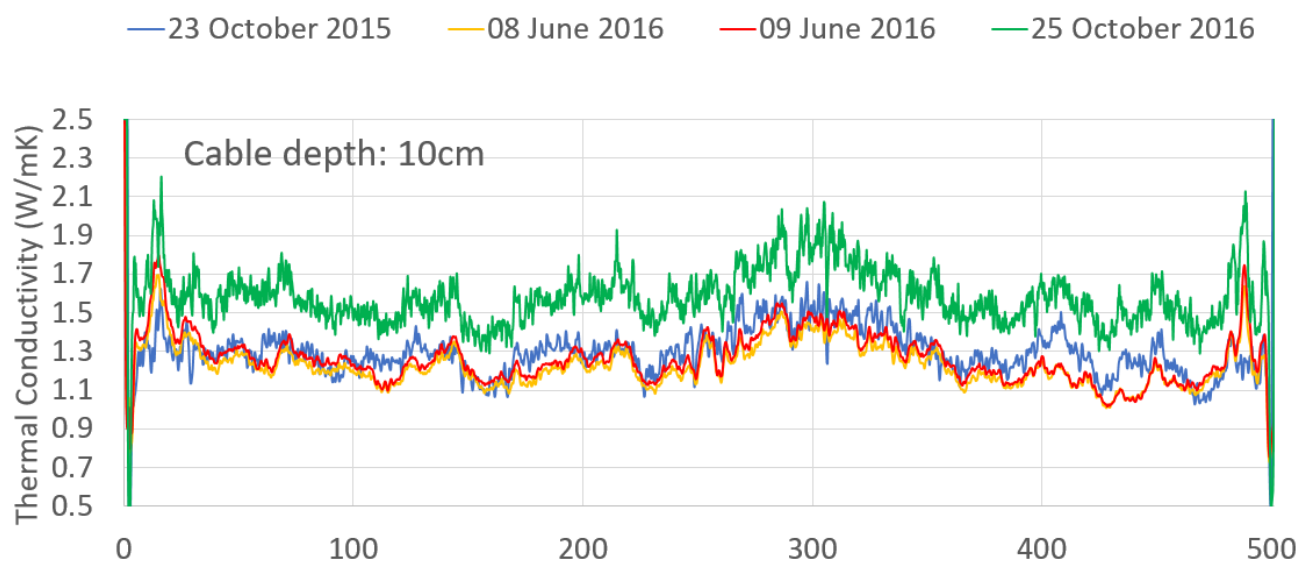


7.7 mm

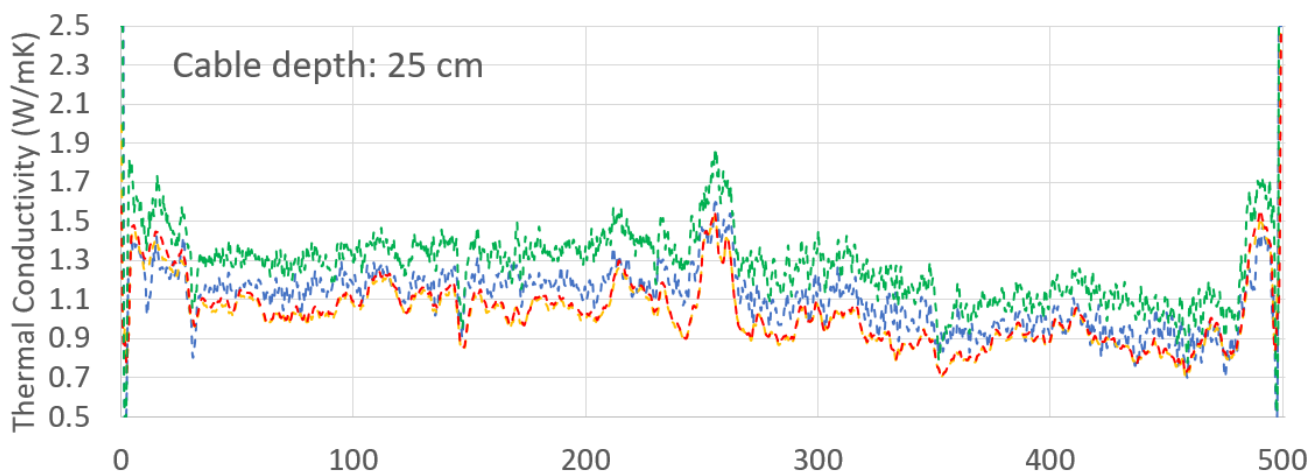




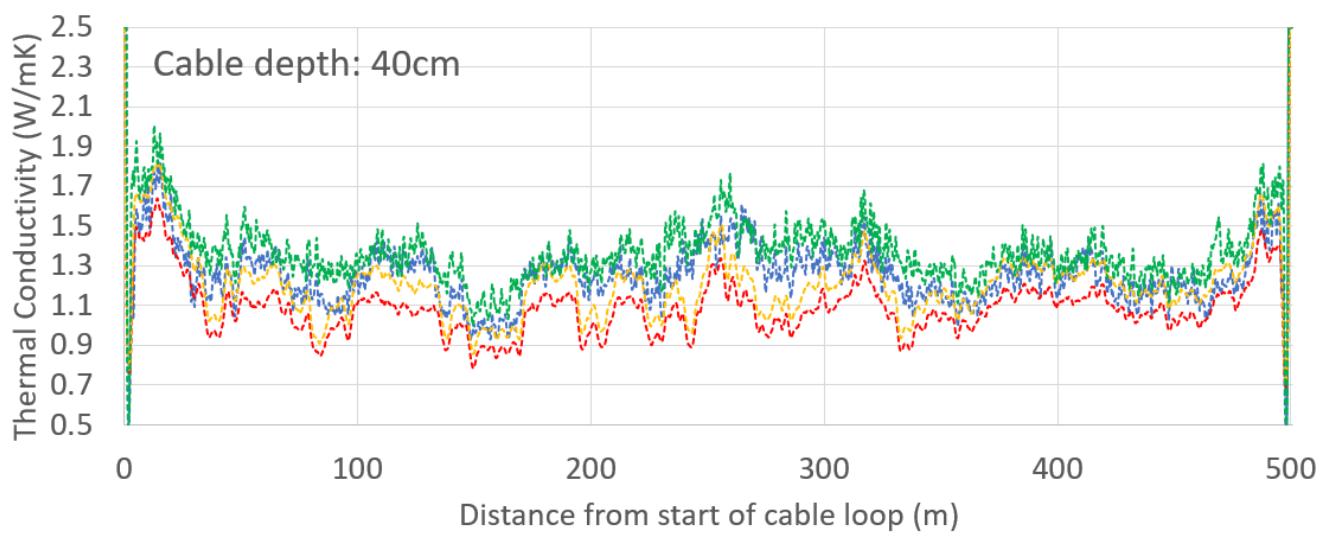
(a)



(b)

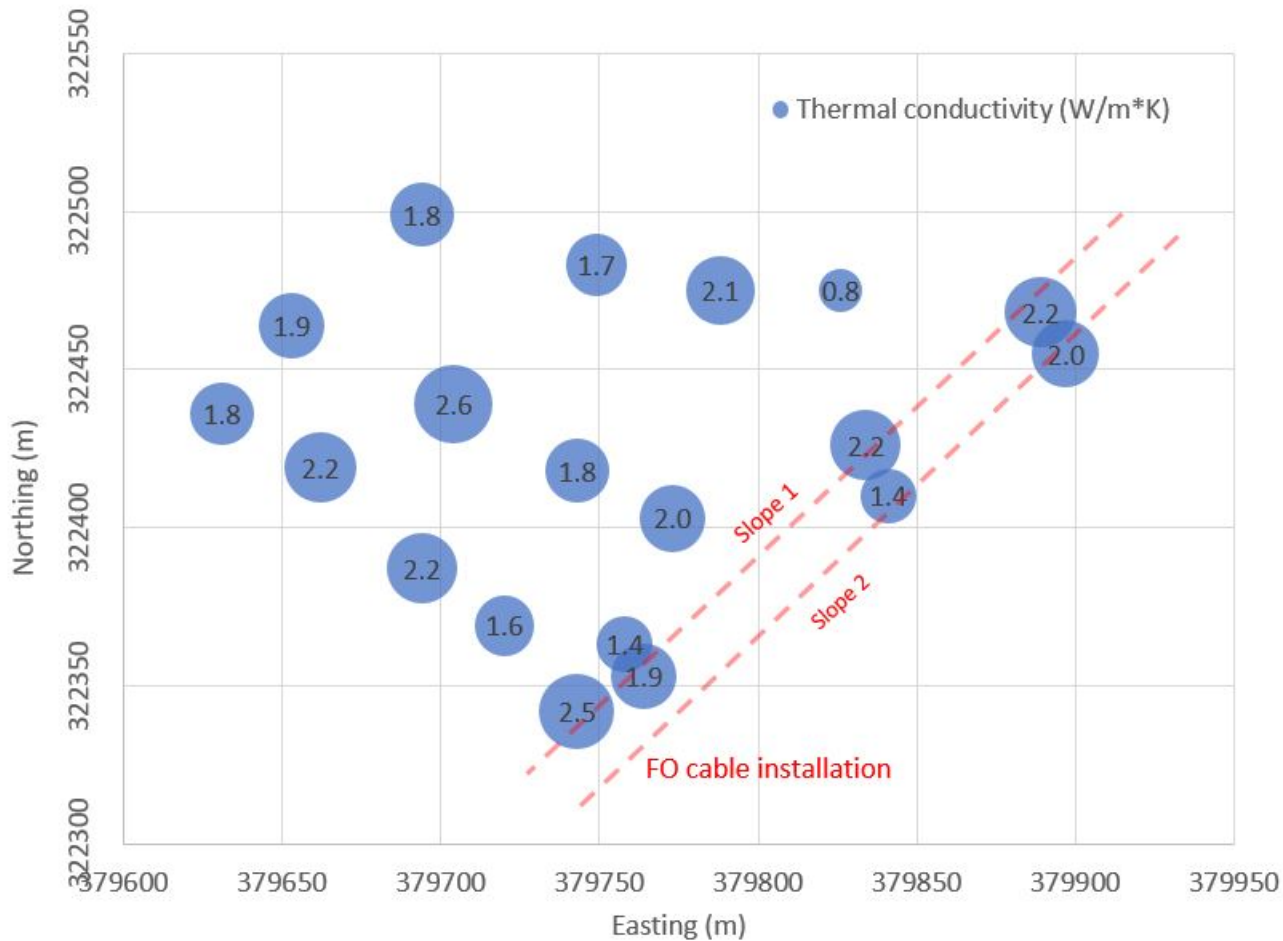


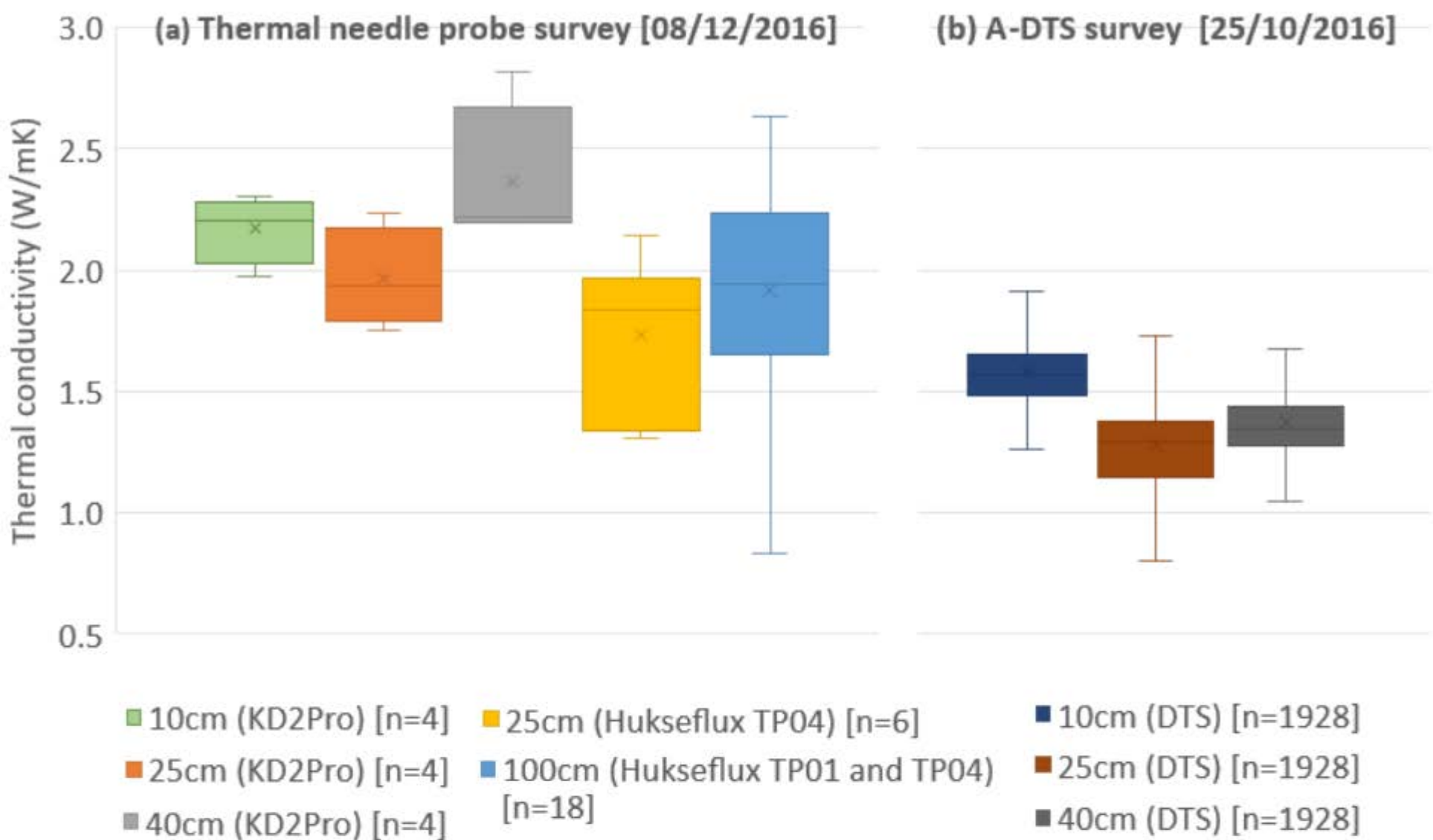
(c)

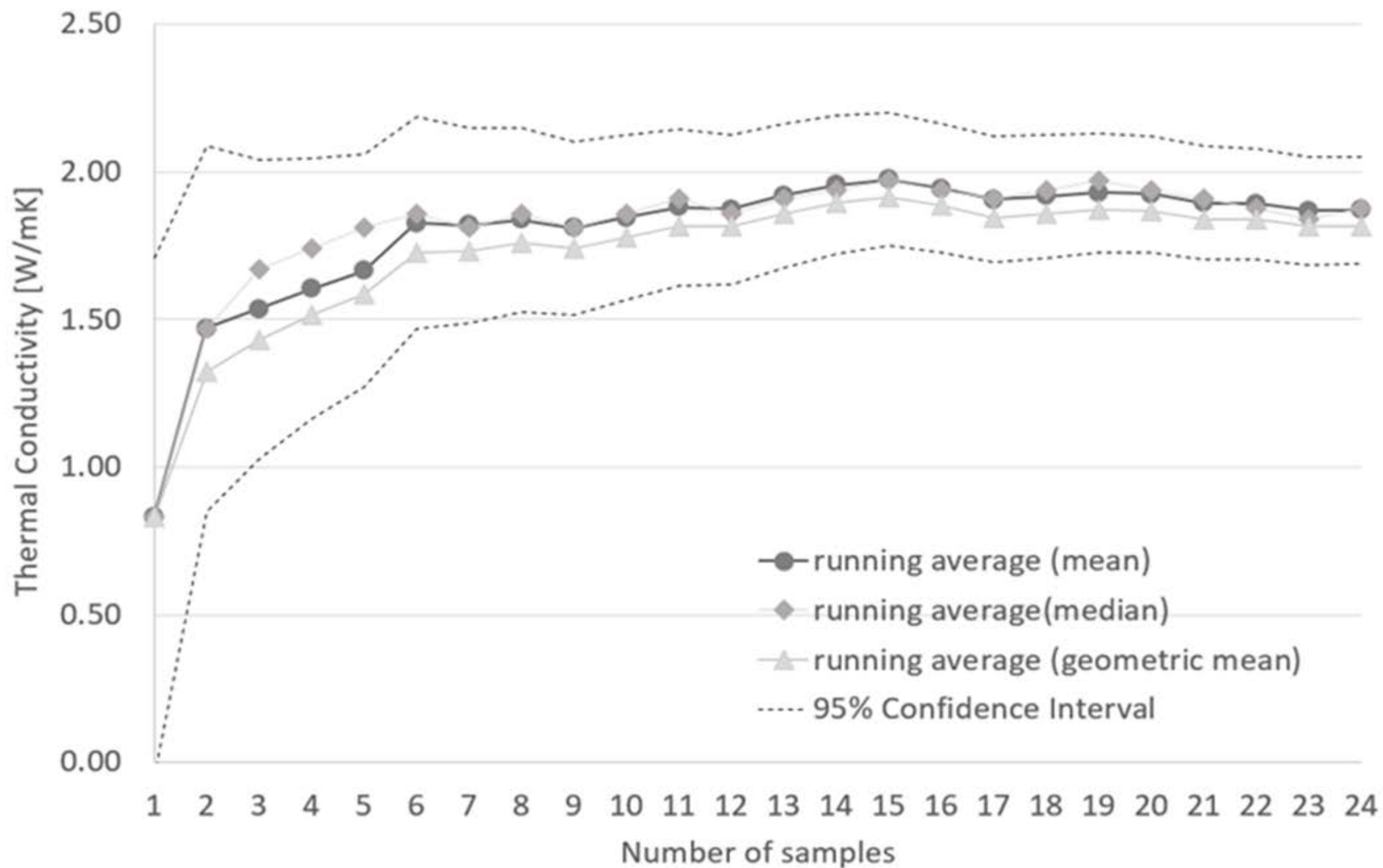












Survey date	Power Density	DTS sampling	DTS time	DTS model
	$Q$		interval	
[dd/mm/yy]	[W m <sup>-1</sup> ]	[m]	[s]	
23/10/15	3.3±1%	0.25	20	XT-DTS
08/06/16	3.7±1%	0.25	10	Ultima-M
09/06/16	4.8±1%	0.25	10	Ultima-M
25/10/16	5.0±1%	0.125	10	Ultima-S



	23/10/2015	08/06/2016	09/06/2016	25/10/2016	Maximum difference in $\lambda$ between campaigns
10cm depth					
n	1928	1928	1928	1928	
Minimum	1.02	1.01	1.02	1.29	0.28
<b>Median</b>	<b>1.29</b>	<b>1.21</b>	<b>1.25</b>	<b>1.56</b>	<b>0.35</b>
Maximum	1.66	1.70	1.80	2.20	0.50
Arithmetic mean	1.30	1.23	1.27	1.58	0.35
Standard deviation	0.11	0.11	0.12	0.14	0.03
<b>Geometric mean</b>	<b>1.29</b>	<b>1.23</b>	<b>1.26</b>	<b>1.57</b>	<b>0.34</b>
25cm depth					
n	1928	1928	1928	1928	
Minimum	0.70	0.70	0.70	0.78	0.08
<b>Median</b>	<b>1.13</b>	<b>1.01</b>	<b>1.02</b>	<b>1.29</b>	<b>0.28</b>
Maximum	1.62	1.53	1.56	1.88	0.35
Arithmetic mean	1.11	1.02	1.03	1.28	0.26
Standard deviation	0.15	0.16	0.16	0.17	0.02
<b>Geometric mean</b>	<b>1.10</b>	<b>1.01</b>	<b>1.02</b>	<b>1.27</b>	<b>0.26</b>
40cm depth					
n	1928	1928	1928	1928	
Minimum	0.93	0.78	0.85	1.00	0.21
<b>Median</b>	<b>1.25</b>	<b>1.09</b>	<b>1.20</b>	<b>1.35</b>	<b>0.26</b>
Maximum	1.83	1.64	1.81	2.01	0.37
Arithmetic mean	1.26	1.09	1.21	1.37	0.28
Standard deviation	0.14	0.13	0.16	0.14	0.03
<b>Geometric mean</b>	<b>1.25</b>	<b>1.08</b>	<b>1.20</b>	<b>1.36</b>	<b>0.28</b>

	(a) Hukseflux (all data)	(b) KD2Pro (all data)	(c) A-DTS 25/10/2016 (all data)
n	24	12	5784
Minimum	0.83	1.76	0.78
<b>Median</b>	<b>1.88</b>	<b>2.02</b>	<b>1.39</b>
Maximum	2.63	2.82	2.02
Arithmetic mean	1.87	2.09	1.41
Standard deviation	0.45	0.27	0.20
<b>Geometric mean</b>	<b>1.82</b>	<b>2.07</b>	<b>1.40</b>